Interleaved Boost Converter with magnetic coupling

Let us consider the physical system shown in Fig. 1. The POG scheme of the Boost Converter

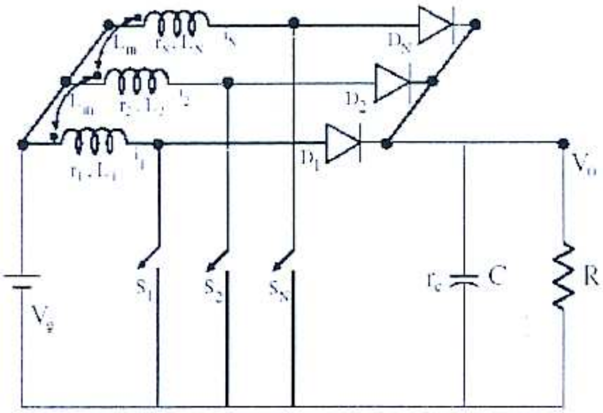

Figura 1: Interleaved Boost Converter with magnetic coupling. The case $m = 3$.

is reported in Fig. 2. where matrices $\mathbf{B}_m$ $\mathbf{L}_m$, $\mathbf{R}_m$, $\mathbf{S}_m$ and $\mathbf{I}_m$ are defined as follows:

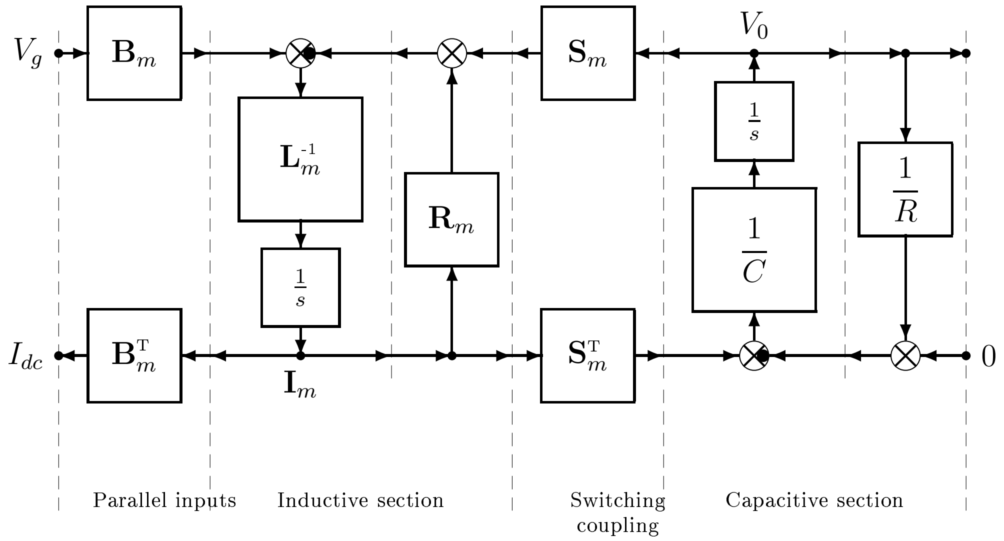

Figura 2: The POG scheme of the Boost Converter shown in Fig. 1 .

$$\mathbf{B}_m = \begin{bmatrix} 1 \\ 1 \\ 1 \\ \vdots \\ 1 \end{bmatrix}, \qquad \mathbf{L}_m = \begin{bmatrix} L_1 & M_{12} & M_{13} & \dots & M_{1m} \\ M_{12} & L_2 & M_{23} & \dots & M_{2m} \\ M_{13} & M_{23} & L_3 & \dots & M_{3m} \\ \vdots & \vdots & \vdots & \ddots & \vdots \\ M_{1m} & M_{2m} & M_{3m} & \dots & L_m \end{bmatrix},$$

and

$$\mathbf{R}_m = \begin{bmatrix} R_1 & 0 & 0 & \dots & 0 \\ 0 & R_2 & 0 & \dots & 0 \\ 0 & 0 & R_3 & \dots & 0 \\ \vdots & \vdots & \vdots & \ddots & \vdots \\ 0 & 0 & 0 & \dots & R_m \end{bmatrix}, \qquad \mathbf{S}_m = \begin{bmatrix} s_1 \\ s_2 \\ s_3 \\ \vdots \\ s_m \end{bmatrix}, \qquad \mathbf{I}_m = \begin{bmatrix} I_1 \\ I_2 \\ I_3 \\ \vdots \\ s_m \end{bmatrix}$$

where s_i are the control inputs:

$$s_i \in \{0,\ 1\}, \qquad\qquad i \in \{1,\ 2,\ 3\}$$

The corresponding state space description is the following:

$$\underbrace{\begin{bmatrix} \mathbf{L}_m & 0 \\ 0 & C \end{bmatrix}}_{\mathbf{L}} \underbrace{\begin{bmatrix} \dot{\mathbf{I}}_m \\ \dot{V}_0 \end{bmatrix}}_{\dot{\mathbf{x}}} = \underbrace{\begin{bmatrix} -\mathbf{R}_m & -\mathbf{S}_m \\ \mathbf{S}_m & -\frac{1}{R} \end{bmatrix}}_{\mathbf{A}} \underbrace{\begin{bmatrix} \mathbf{I}_m \\ V_0 \end{bmatrix}}_{\mathbf{x}} + \underbrace{\begin{bmatrix} \mathbf{B}_m \\ 0 \end{bmatrix}}_{\mathbf{B}} \underbrace{[V_g]}_{\mathbf{u}} \tag{1}$$

that is, in a compact form:

$$\mathbf{L}\,\dot{\mathbf{x}} = \mathbf{A}\,\mathbf{x} + \mathbf{B}\,\mathbf{u}$$

The energy stored in the system E_s and the dissipating power P_d can be easily computed as follows:

$$E_s = \frac{1}{2}\mathbf{x}^{\mathrm{T}}\,\mathbf{L}\,\mathbf{x}, \qquad\qquad P_d = \mathbf{x}^{\mathrm{T}}\,\mathbf{A}\,\mathbf{x}$$

The POG scheme of the Boost Converter when $m = 3$ is shown in Fig. 1 is shown in Fig. 3.

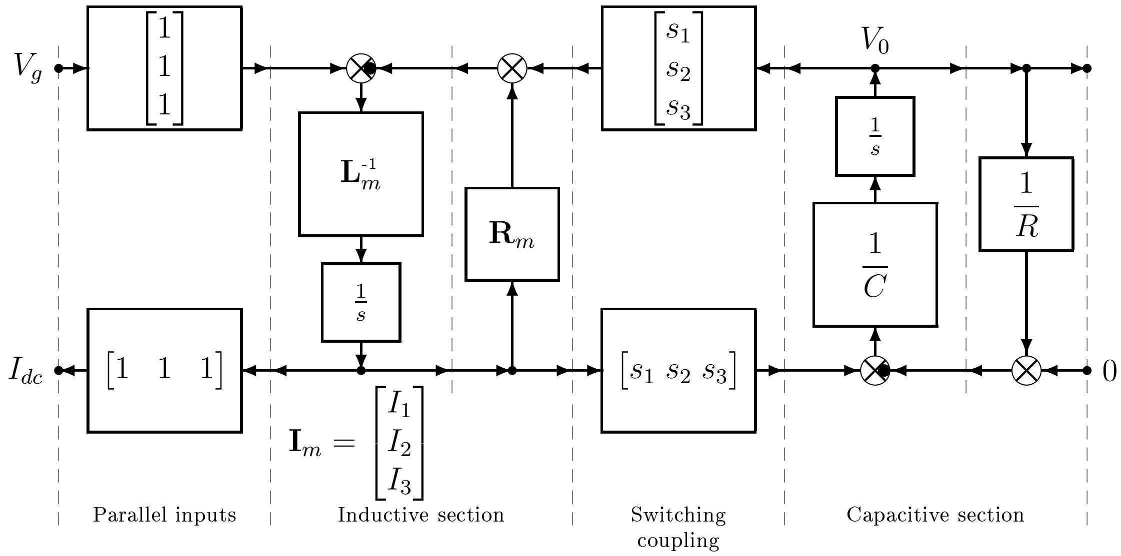

Figura 3: The POG scheme of the Boost Converter shown in Fig. 1 ($m = 3$).

From Fig. 3 it is straightforward to obtain the state space description of the POG scheme:

$$\left[\begin{array}{ccc|c} L_1 & M_{12} & M_{13} & 0 \\ M_{12} & L_2 & M_{23} & 0 \\ M_{13} & M_{23} & L_3 & 0 \\ \hline 0 & 0 & 0 & C \end{array}\right] \left[\begin{array}{c} \dot{I}_1 \\ \dot{I}_2 \\ \dot{I}_3 \\ \hline \dot{V}_0 \end{array}\right] = \left[\begin{array}{ccc|c} -R_1 & 0 & 0 & -s_1 \\ 0 & -R_2 & 0 & -s_2 \\ 0 & 0 & -R_3 & -s_3 \\ \hline s_1 & s_2 & s_3 & -\frac{1}{R} \end{array}\right] \left[\begin{array}{c} I_1 \\ I_2 \\ I_3 \\ \hline V_0 \end{array}\right] + \left[\begin{array}{c} 1 \\ 1 \\ 1 \\ \hline 0 \end{array}\right] [V_g] \tag{2}$$

The POG scheme of Fig. 3 has been introduced in Simulink and the corresponding block diagram is shown in Fig. 4.

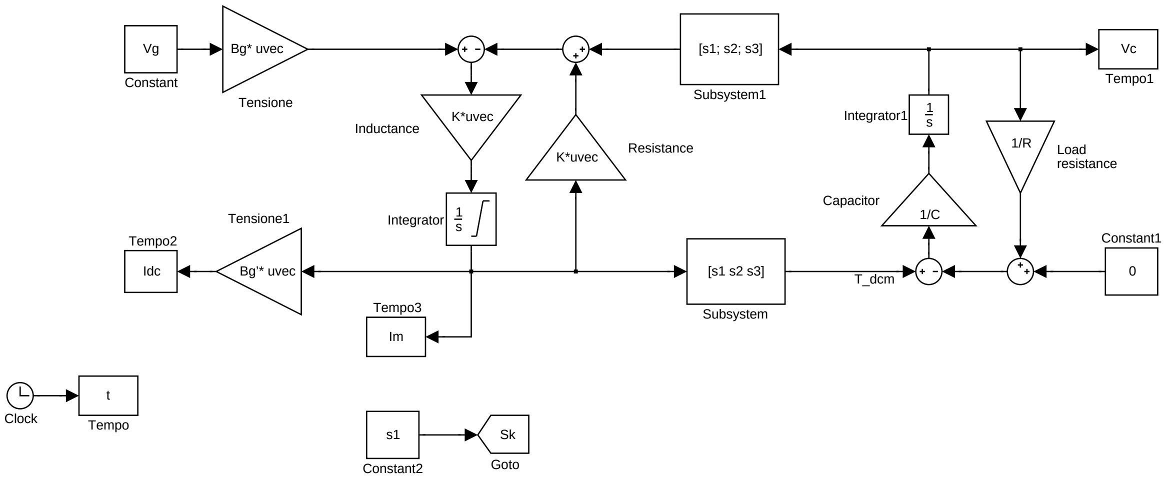

Figura 4: The Simulink block diagram of the POG scheme shown in Fig. 3.

When $m = 1$ one obtains the following simplified model:

$$\left\{ \begin{array}{rcl} L_1 \dot{I}_1 & = & -R_1 I_1 - s_1 V_0 + V_g \\ C\dot{V}_0 & = & s_1 I_1 - \frac{1}{R} V_0 \end{array} \right. \tag{3}$$

In matrix form it can be described as follows:

$$\left[\begin{array}{c|c} L_1 & 0 \\ \hline 0 & C \end{array} \right] \begin{bmatrix} \dot{I}_1 \\ \dot{V}_0 \end{bmatrix} = \left[\begin{array}{c|c} -R_1 & -s_1 \\ \hline s_1 & -\frac{1}{R} \end{array} \right] \begin{bmatrix} I_1 \\ V_o \end{bmatrix} + \begin{bmatrix} 1 \\ 0 \end{bmatrix} V_g \tag{4}$$

When $s_1 = 0$ the two dynamic elements are de-coupled:

$$\left\{ \begin{array}{rcl} L_1 \dot{I}_1 & = & -R_1 I_1 + V_g \\ C\dot{V}_0 & = & -\frac{1}{R} V_0 \end{array} \right. \quad \Rightarrow \quad \left\{ \begin{array}{rcl} I_1(t) & = & e^{-\frac{R_1}{L_1}t} I_{10} + \frac{V_g}{R_1} \left[1 - e^{-\frac{R_1}{L_1}t} \right] \\ V_0(t) & = & e^{-\frac{t}{RC}} V_0 \end{array} \right.$$

In this case the steady-state point is $(I_1,\ V_0) = (\frac{V_g}{R_1},\ 0)$ and the corresponding state space trajectories are shown in Fig. 5, see Matlab/Simulink files “Boost.m” e “Boost_mdl.mdl”. When $s_1 = 1$ the two dynamic elements are coupled:

$$\left\{ \begin{array}{rcl} L_1 \dot{I}_1 & = & -R_1 I_1 - V_0 + V_g \\ C\dot{V}_0 & = & I_1 - \frac{1}{R} V_0 \end{array} \right.$$

and the steady-state point is $(I_1,\ V_0) = (\frac{V_g}{R_1+R},\ \frac{V_g R}{R_1+R})$. The corresponding state space trajectories are shown in Fig. 6.

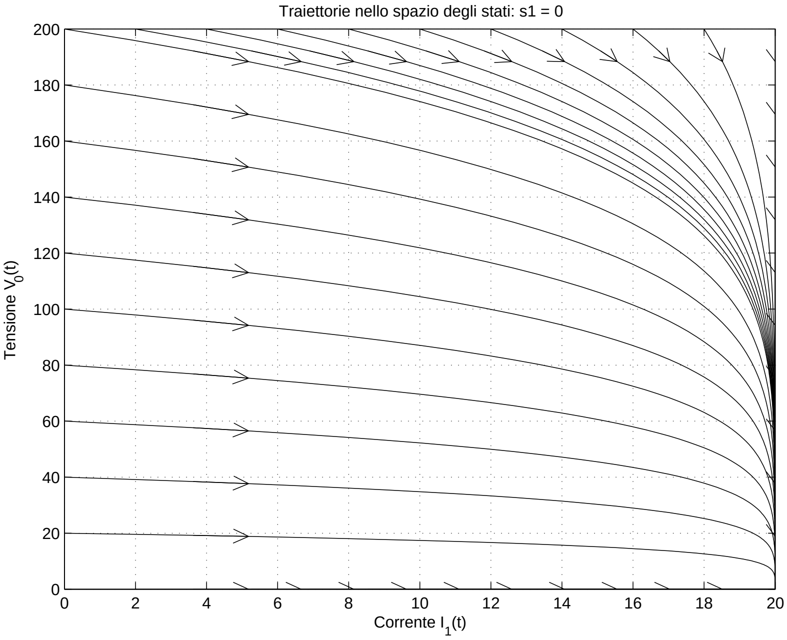

Figura 5: State space trajectories when $s_1 = 0$.

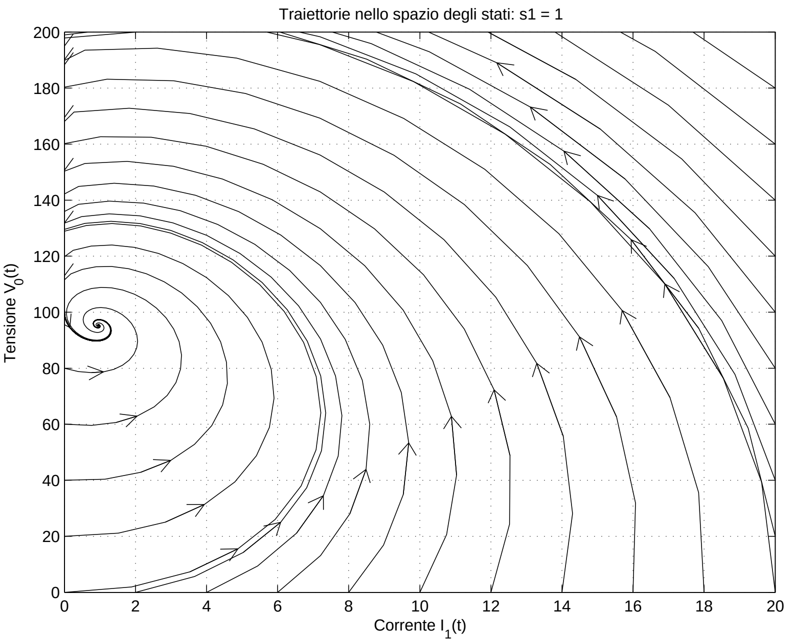

Figura 6: State space trajectories when $s_1 = 1$.

Feedforward control

Let control system (3) with a constant duty cycle $\bar{s}_1 \in [0, 1]$. The steady-state conditions can be obtained from (4) when $\dot{I}_0$ and $\dot{V}_0 = 0$:

$$\left[\begin{array}{c|c} -R_1 & -\bar{s}_1 \\ \hline \bar{s}_1 & -\frac{1}{R} \end{array}\right] \begin{bmatrix} I_1 \\ V_0 \end{bmatrix} + \begin{bmatrix} 1 \\ 0 \end{bmatrix} V_g = 0 \qquad \rightarrow \qquad \begin{bmatrix} I_1 \\ V_0 \end{bmatrix} = - \left[\begin{array}{c|c} -R_1 & -\bar{s}_1 \\ \hline \bar{s}_1 & -\frac{1}{R} \end{array}\right]^{-1} \begin{bmatrix} 1 \\ 0 \end{bmatrix} V_g$$

from which one obtains

$$\begin{bmatrix} I_1 \\ V_0 \end{bmatrix} = -\frac{R}{R_1 + R\,\bar{s}_1^2} \left[\begin{array}{c|c} -\frac{1}{R} & \bar{s}_1 \\ \hline -\bar{s}_1 & -R_1 \end{array}\right] \begin{bmatrix} V_g \\ 0 \end{bmatrix} = \frac{1}{R_1 + R\,\bar{s}_1^2} \begin{bmatrix} V_g \\ \bar{s}_1\, R\, V_g \end{bmatrix}$$

If $V_g = 100$ V, $\bar{s}_1 = 0.5$, $R_1 = 5$ Ohm and $R = 100$ Ohm, the steady-state point is:

$$\begin{bmatrix} I_1 \\ V_0 \end{bmatrix} = \begin{bmatrix} 3.33 \text{ A} \\ 166.66 \text{ V} \end{bmatrix}$$

The simulation results obtained with these parameters (see files "Boost_Duty_Cycle_R100.m" and "Boost_Duty_Cycle_R100_mdl.mdl") are shown in Figg. 7 and 8.

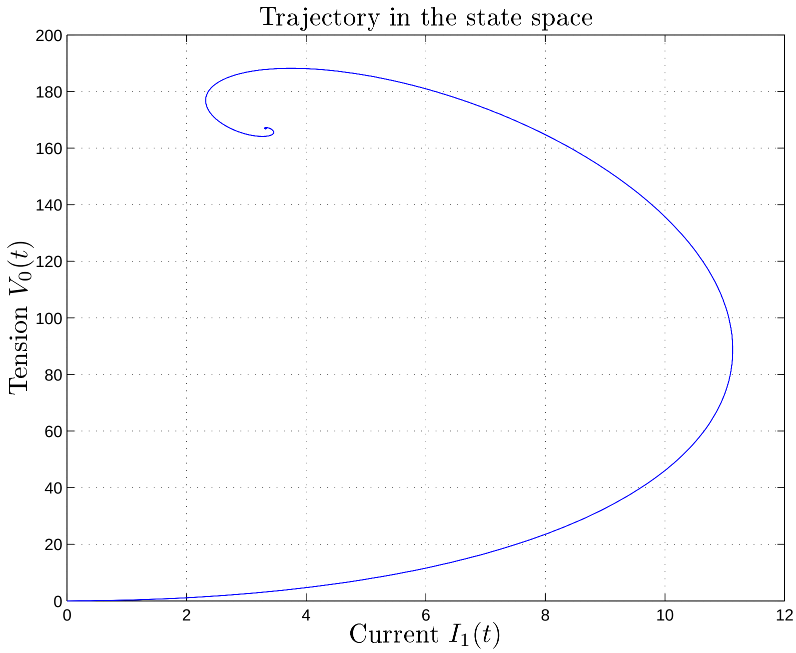

Figura 7: State space trajectories when $\bar{s}_1 = 0.5$.

The simulation results shown in Fig. 9 (see files "Boost_Duty_Cycle.m" and "Boost_Duty_Cycle_mdl.mdl") have been obtained by using the following parameters:

$$R_1 = 0.1 \text{ Ohm}, \qquad \text{and} \qquad R = 19.9 \text{ Ohm}$$

In this case the steady-state point is:

$$\begin{bmatrix} I_1 \\ V_0 \end{bmatrix} = \begin{bmatrix} 19.7 \text{ A} \\ 196.1 \text{ V} \end{bmatrix}$$

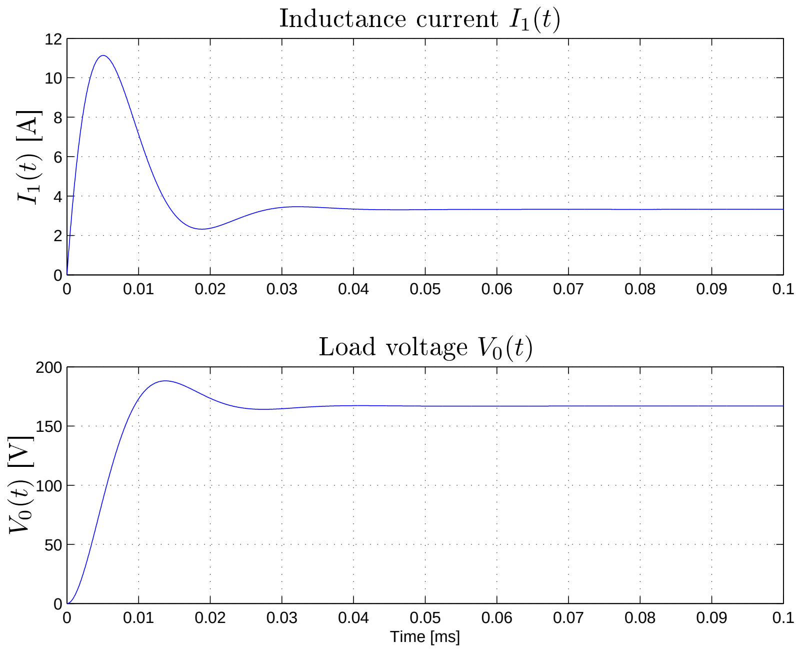

Figura 8: Inductance current $I_1(t)$ and load voltage V_0 when $\bar{s}_1 = 0.5$.

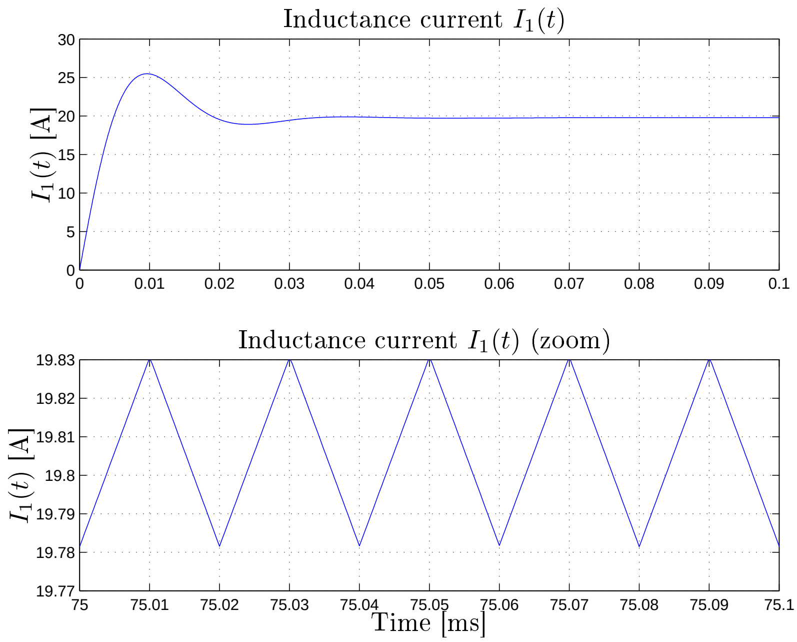

Figura 9: Inductance current $I_1(t)$ when $R_1 = 0.1$ Ohm and $R = 19.9$ Ohm .

For the simulation of an Interleaved Boost Converter of order m with all independent parameters please refer to files "Boost_of_order_M.m" and "Boost_of_order_M_mdl.mdl". In Figg. 10, 11 and 12 are shown the simulation results obtained with the following parameters: number of inductors $m = 3$; input voltage $V_g = 100$ V; main capacitor $C = 200\ \mu$F; load resistance $R = 20$ Ohm; self inductance coefficients $[L_1,\ L_2,\ L_3] = [20,\ 18,\ 22]$ mH; resistances of the inductors $[R_1,\ R_2,\ R_3] = [1,\ 3,\ 2]$ Ohm; duty cycles $[\bar{s}_1,\ \bar{s}_2,\ \bar{s}_3] = [0.5,\ 0.45,\ 0.48]$. The mutual inductance coefficients M_{ji} between inductors L_i and L_j have been defied as follows:

$$M_{ji} = M_c\sqrt{L_i\, L_j}$$

where $0 < M_c < 1$ is a proper positive coefficient. For the m-order case, the steady-state variables can be computed as follows, see eq. (2):

$$\begin{bmatrix} I_1 \\ I_2 \\ I_3 \\ \hline V_0 \end{bmatrix} = -\left[\begin{array}{ccc|c} -R_1 & 0 & 0 & -s_1 \\ 0 & -R_2 & 0 & -s_2 \\ 0 & 0 & -R_3 & -s_3 \\ \hline s_1 & s_2 & s_3 & -\frac{1}{R} \end{array}\right]^{-1} \begin{bmatrix} 1 \\ 1 \\ 1 \\ \hline 0 \end{bmatrix} [V_g] = \begin{bmatrix} 7.81 \text{ A} \\ 5.67 \text{ A} \\ 5.75 \text{ A} \\ 184.38 \text{ V} \end{bmatrix}$$

The reported numerical values refer to the considered particular case.

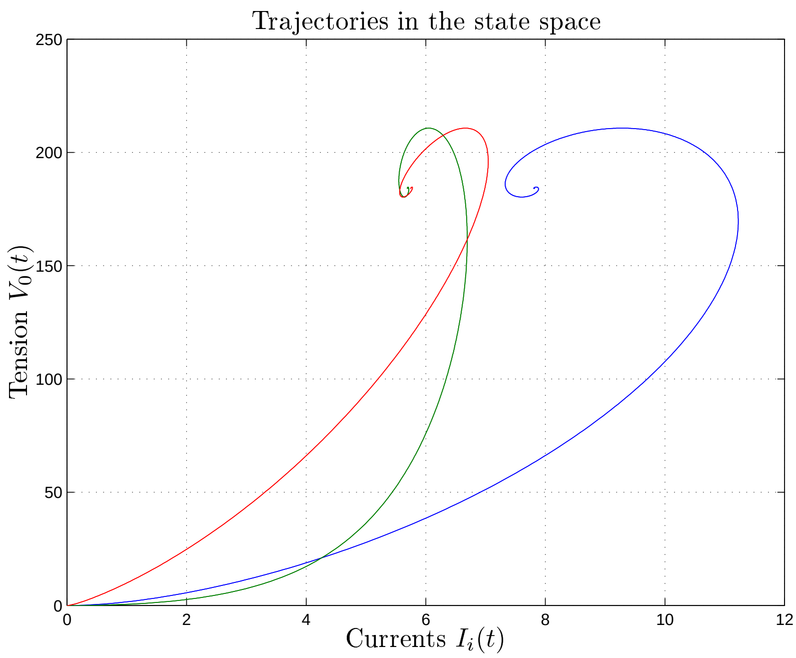

Figura 10: State space trajectories for the considered 3-th order case.

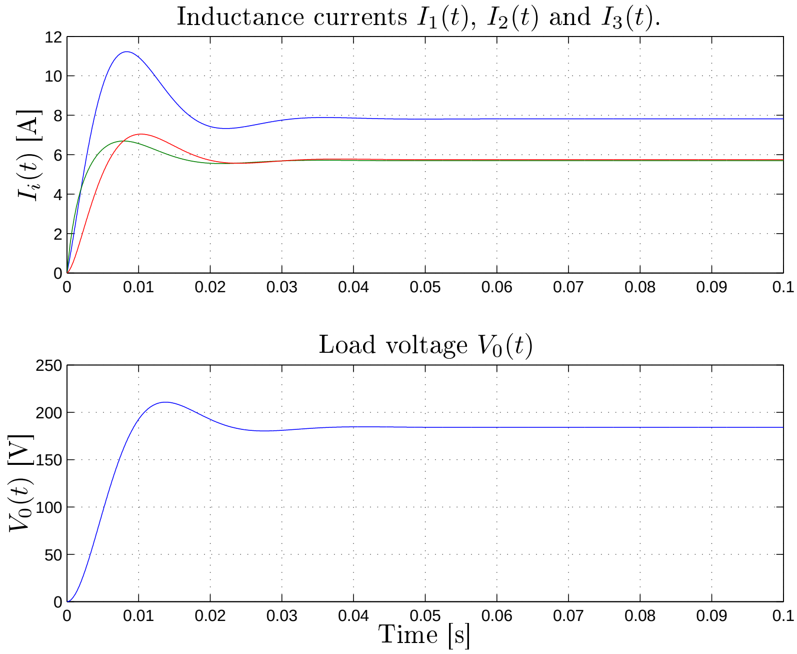

Figura 11: Inductance currents $I_1(t)$, $I_2(t)$, $I_3(t)$ and load voltage V_0.

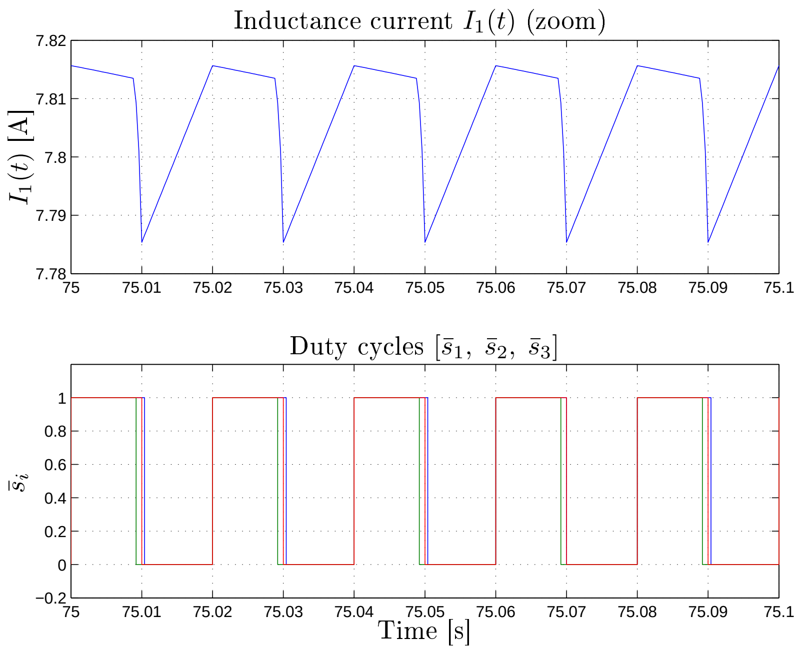

Figura 12: Inductance currents $I_1(t)$, $I_2(t)$, $I_3(t)$ and load voltage V_0.

Feedback control

Let V_{ref} denote the desired output voltage and let us consider the following control law:

$$\lambda(V_0) = V_{ref} - V_0 \qquad \Rightarrow \qquad s_1 = \frac{1 + \mathrm{sign}(\lambda(V_0))}{2} = \begin{cases} 1 & \text{if} \quad \lambda(V_0) \geq 0 \\ 0 & \text{if} \quad \lambda(V_0) < 0 \end{cases}$$

The obtained trajectories in the $(I_1,\ V_0)$ state space are shown in Fig. 13, see Matlab/Simulink files "Boost_3.m" e "Boost_3_mdl.mdl". The dynamics of the system when the sliding

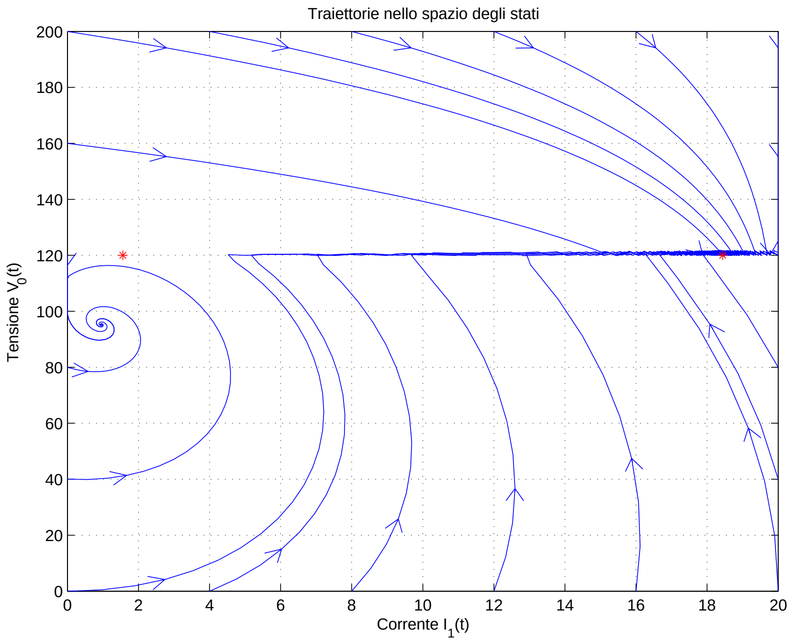

Figura 13: State space trajectories when the control $s_1 = \frac{1+\mathrm{sign}(\lambda(V_0))}{2}$ is used.

surface $\lambda(V_0) = V_{ref} - V_0 = 0$ is reached is obtained by imposing $\dot{\lambda}(V_0) = 0$:

$$\dot{V}_0 = 0 \qquad \rightarrow \qquad s_1 I_1 - \frac{1}{R} V_{ref} = 0 \qquad \rightarrow \qquad s_1 = \frac{V_{ref}}{R\, I_1} = \bar{s}_1$$

The control variable $s_1 \in \{0,\ ,1\}$ theoretically switches at infinite frequency with duty-cycle equal to $\bar{s}_1 \in [0,\ 1]$. The duty-cycle cannot exceed the maximum value:

$$\bar{s}_1 < 1 \qquad \rightarrow \qquad \boxed{I_1 > \frac{V_{ref}}{R}}$$

When parameters R and I_1 change, the duty-cycle $\bar{s}_1$ changes such to guarantee that $V_0 = V_{ref}$. Substituting $\bar{s}_1$ in the first equation of system (3) one obtains:

$$\dot{I}_1 = -\frac{R_1 I_1}{L_1} - \frac{V_{ref}^2}{R\, L_1\, I_1} + \frac{V_g}{L_1} \tag{5}$$

The equilibrium points of this nonlinear differential equation are obtained when $\dot{I}_1 = 0$:

$$R_1 R\, I_1^2 - V_g R\, I_1 + V_{ref}^2 = 0 \qquad \rightarrow \qquad I_{1,2}^* = \frac{V_g R \mp \sqrt{V_g^2 R^2 - 4\, R_1 R V_{ref}^2}}{2\, R_1 R}$$

The equilibrium points are real only if:

$$V_g^2 R^2 - 4\, R_1 R V_{ref}^2 > 0 \qquad \rightarrow \qquad \boxed{V_{ref} < \sqrt{\frac{R}{4R_1}}\, V_g}$$

In Fig. 14 it has been reported the qualitative behaviour of $\dot{I}_1$ as a function of current I_1,

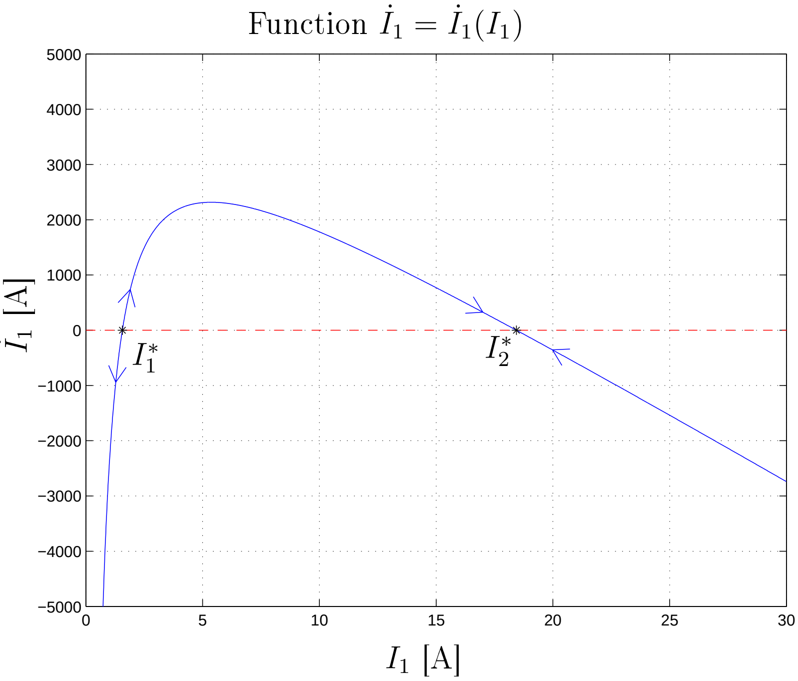

Figura 14: Qualitative behaviour of $\dot{I}_1$ as a function of current I_1.

see eq. (5). From this figure it is evident that the equilibrium point I_1^* is unstable, while the equilibrium point I_2^* is stable.